PCCP

PAPER

View Article Online
View Journal | View Issue

Cite this: *Phys. Chem. Chem. Phys.*, 2018, **20**, 12992

Gold-doped silver nanoclusters with enhanced photophysical properties†

Dinesh Mishra,[a] Vladislav Lobodin,[b] Chengqi Zhang,[a] Fadi Aldeek,[a] Eric Lochner[c] and Hedi Mattoussi*[a]

Received 29th December 2017,
Accepted 13th April 2018

DOI: 10.1039/c7cp08682b

rsc.li/pccp

We detail the characterization of atomically precise, luminescent silver and gold bimetallic nanoclusters (Ag and AgAuNCs) grown in the presence of bidentate lipoic acid (LA, the oxidized form) and dihydrolipoic acid (DHLA, the reduced form) ligands. We found that while doping AuNCs with Ag or Cu precursors using up to a 50% molar fraction (during growth) did not lead to any photoluminescence enhancement, doping of AgNCs with Au resulted in a six-fold enhancement of the PL emission compared to undoped AgNCs. The effect of doping is also reflected in the optical absorption and PL excitation spectra of the gold-doped NCs (AgAuNCs), where a clear blue shift in the absorbance features with respect to the pure AgNCs has been measured. Mass spectrometry measurements using ESI-MS showed that the AgNCs and Au-doped AgNCs had the compositions $Ag_{29}(DHLA)_{12}$ and $Ag_{28}Au(DHLA)_{12}$, respectively. The bimetallic nature of the AgAuNC cores was further supported by X-ray Photoelectron Spectroscopy (XPS) measurements. Data showed that the binding energies of the Ag and Au atoms measured from the nanoclusters were shifted with respect to those of the Ag and Au metals. Furthermore, the change in the Ag binding energy was affected by the presence of Au atoms. DOSY-NMR measurements performed on both sets of nanoclusters yielded no change in the hydrodynamic radius measured for either set of NCs when capped with the same ligands.

Introduction

Atomically precise nanoclusters made of gold and silver cores (AuNCs and AgNCs) raise several important fundamental physical and chemical questions, and they have very promising applications in sensing, imaging and catalysis.[1–7] Due to their ultra-small core size (diameter < 2 nm), these NCs have a finite number of atoms and exhibit molecule-like properties with discrete electronic states arising from carrier confinement effects.[8] They constitute a bridge between discrete molecules and colloidal nanoparticles. Over the past two decades, an intense effort has been focused on the growth and characterization of fluorescent metal NCs.[7] Also, there have been several reports on their use in targeted bio-medical applications.[9–15]

The optical absorption of known magic size NCs exhibits size- and ligand-dependent features.[16–18] In contrast, there is no clear relation between the core size of the NC and the measured optical emission. Additionally, such emissions can be affected by the nature of the surface ligands used for preparing the NCs.[15,19] Indeed, it has been shown in several studies that it is possible to change the optical emission of noble metal NCs (Au and Ag, in particular) by varying the nature and size of capping ligands such as polymers, biomolecules (peptides, proteins, DNA, *etc.*) and thiolates.[12,19–24] It has also been suggested that photoemission from these materials may arise from the electronic transitions in the metallic core (singlet–singlet), or equally involve a ligand-to-metal charge transfer (LMCT) occurring at the surface. The latter is associated with a large stokes shift combined with a rather long fluorescence lifetime.[25] Yet, no clear origin of the PL emission has been unequivocally identified for these materials.

An alternative approach that is gaining increasing interest is to "dope" the NCs with transition metal atoms (*e.g.*, Au, Ag, Pt, Pd, and Cu) as a means of controlling and/or improving the electronic and photophysical properties of the final product. Using this strategy, several bimetallic NCs with a composition of M_xN_y have been prepared, where M and N designate the metal atoms and x and y represent the respective numbers of those atoms.[14,26–29] Doping can be achieved either by the reduction of a mixture of the two metal precursors in the presence of ligands, or by cation exchange methods.[27,28,30] The latter involves the substitution of a certain number of atoms in a NC with the doping metal of choice.[30]

Among a wide variety of ligands used for preparing monolayer-protected Au and Ag nanoclusters, thiolates have

[a] *Florida State University, Department of Chemistry and Biochemistry, 95 Chieftan Way, Tallahassee, FL 32306, USA. E-mail: mattoussi@chem.fsu.edu*
[b] *National High Magnetic Field Laboratory, Tallahassee, FL, 32306, USA*
[c] *Florida State University, CMMP, Department of Physics, 77 Chieftan Way, Tallahassee, FL 32306, USA*

† Electronic supplementary information (ESI) available: Experimental details, additional absorption profiles, mass spectrometry data, and colloidal stability data. See DOI: 10.1039/c7cp08682b

been the most ubiquitous, due to their strong coordination interactions with gold and silver surfaces. Several thiolate-capped magic size NCs made of Au and Ag cores with emission from the blue to the NIR region of the spectrum have been reported.[11,31–34] Bidentate lipoic acid (LA) and its reduced form (dihydrolipoic acid, DHLA) have been used to prepare fluorescent gold and silver NCs. We, as well as others, have reported on the growth of red-emitting LA-capped Au and AgNCs.[22,35–39] Interestingly, AuNCs and AgNCs grown using this ligand have always exhibited optical absorption features that are largely independent of the growth conditions used by various groups, though variation in the PL emission maxima have been reported.[22,37,39,40] Independent studies from groups led by Nienhaus and Wang proposed the composition of the AuNCs to be Au_{22}, based on the resemblance of their optical absorption to previously reported Au_{22} NCs.[38,41] However, there are variations in the reported atomic compositions of the AgNCs. For example, Banerjee and co-workers reported the presence of Ag_4 and Ag_5 species whereas Meijerink and co-workers suggested the formation of Ag_{25} NCs.[35,39] A recent detailed study by Antoine and co-workers identified NCs with the stoichiometry $Ag_{29}DHLA_{12}$ and further investigated the one and two-photon fluorescence properties of such materials. They found that two different emission colors are generated in a two-photon excitation mode.[36] Ag_{29} NCs have also been prepared in organic solution by Bakr and co-workers, using 1,3 benzenedithiol and triphenylphosphine as ligands.[42] The authors have identified the crystal structure and the electronic states using a combination of X-ray diffraction and DFT calculations. In a recent study, they reported a 26-fold enhancement of the PL quantum yield of these NCs upon doping with Au atoms.[29]

In this study, we investigate the growth of bimetallic NCs in aqueous phase by co-reduction of the metal precursors (*i.e.* Au, Ag and Cu) in the presence of bidentate LA/DHLA ligands using sodium borohydride. We find that the best quality nanoclusters (highest PL emission) are obtained when a small fraction of Au atoms is inserted into the core structure of the AgNCs. Measured enhancement of the PL quantum yield of these bimetallic NCs reached six-fold (from ~3% to ~20%) without any measurable shift in the PL maximum. This is accompanied by a progressive change in the absorption with a blue shift in the absorption maximum relative to the pure AgNCs. In addition, we show that functionalization of these NCs can be achieved using end-functionalized polyethylene glycol (PEG) appended-DHLA (DHLA-PEG-R) during the growth step.

Experimental section

Materials

Lipoic acid (99%), tetrachloroauric acid trihydrate (99.9%), anhydrous copper sulfate (99.99%), sodium borohydride (99.99%, granular), polyethylene glycol (M_w = 600 g mol^{-1}) and polyethylene glycol methyl ether (M_w = 750 g mol^{-1}), didodecyldimethylammonium bromide (DDAB) and organic solvents were purchased from Sigma Aldrich (St Louis, MO). Silver nitrate (99.9%) was purchased from Alfa-Aesar (Ward Hill, MA). Solutions were prepared in DI water (nanopure, 18 MΩ). All chemicals and solvents were used as purchased, without further purification, unless otherwise specified.

Ligand synthesis

LA-PEG ligands with $-OCH_3$, $-NH_2$ and $-COOH$ terminal groups were synthesized following the protocols described in previous reports.[43,44] Briefly, to synthesize LA-PEG-OCH_3, the hydroxyl terminal group of HO-PEG-OCH_3 was first modified to azide, followed by reduction to amine using triphenylphosphine. The amine-PEG ligand was then linked to lipoic acid using dicyclohexylcarbodiimide (DCC) coupling. LA-PEG-NH_2 was prepared by first modifying the hydroxyl terminal groups of a HO-PEG-OH chain to azides, followed by reduction of one azide to amine using triphenylphosphine, and then coupling to LA using DCC. This yielded an azide-terminated ligand, LA-PEG-N_3, which was further reduced to LA-PEG-NH_2 using triphenylphosphine. The $-NH_2$ terminated ligand was reacted with succinic anhydride to form LA-PEG-COOH ligand.[43] Chemical reduction of LA and LA-PEG to DHLA and DHLA-PEG, respectively, was carried out in ethanol using $NaBH_4$.[43,44]

Growth of copper- and silver-doped AuNCs (route 1)[37]

The AuNCs and bimetallic Au/Ag and Au/Cu NCs were prepared under mild alkaline conditions following the method reported by our group for growing AuNCs.[37] In a typical reaction, 7.5 μmoles of lipoic acid (LA, the oxidized form of the ligand) was dissolved in 5 mL of water containing 12.5 μL of 2 M NaOH. Then, aqueous solutions of $HAuCl_4{\cdot}3H_2O$ and $AgNO_3$ or $HAuCl_4{\cdot}3H_2O$ and $CuSO_4$ (both with a concentration of 50 mM) were added stepwise. We varied the molar fraction of silver or copper precursors from 0 to ~50%, while keeping the total volume of the metal precursors fixed at 50 μL and maintaining the overall metal-to-ligand molar ratio at 1:3 (this ratio was used in ref. 37); the amounts of precursor solutions used are provided in Table 1. After stirring the mixture for 5 minutes, 100 μL of 50 mM $NaBH_4$ was added dropwise and the mixture was left stirring overnight (~15 hours). The resulting clusters were purified using a membrane filtration device from Millipore (with cutoff M_W = 10 kDa) and stored in the dark at 4 °C until further use.

Growth of copper- and silver-doped AuNCs (route 2)[45]

Here, the growth of Ag or Cu-doped Au NCs was carried out under strong alkaline conditions, following the procedure reported by Xie and coworkers.[45] Briefly, 200 μL of 50 mM solution of DHLA (prepared in methanol) was dissolved in 4.5 mL DI water. Then, aqueous solutions of $HAuCl_4{\cdot}3H_2O$ and $AgNO_3$ or $HAuCl_4{\cdot}3H_2O$ and $CuSO_4$ were added stepwise.

Table 1 Conditions used to grow Ag- and Cu-doped AuNCs following the protocol in ref. 37. Metal : ligand ratio = 1 : 3; [$NaBH_4$] = 100 μL (50 mM); [NaOH] = 12.5 μL (2 M); reaction time ~15 hours

$HAuCl_4{\cdot}3H_2O$ (50 mM)	50 μL	47.5 μL	45 μL	37.5 μL	25 μL
$AgNO_3/CuSO_4$ (50 mM)	—	2.5 μL	5 μL	12.5 μL	25 μL

Table 2 Conditions used to grow Ag- and Cu-doped AuNCs following the protocol in ref. 45. Metal : ligand ratio = 1 : 2; [$NaBH_4$] = 100 μL (113 mM); [NaOH] = 150 μL (2 M); reaction time ~3 hours

$HAuCl_4 \cdot 3H_2O$ (50 mM)	100 μL	95 μL	90 μL	75 μL	50 μL
$AgNO_3/CuSO_4$ (50 mM)	—	5 μL	10 μL	25 μL	50 μL

The molar fraction of Ag precursor was varied from 0 to ~50%; the amounts of precursor solutions used are provided in Table 2. The metal-to-ligand ratio was maintained at 1 : 2 (this ratio was used in ref. 45). This mixture was stirred for 3–5 min, yielding a cloudy solution of metal thiolate complexes, which was completely solubilized by addition of 150 μL of 2 M NaOH solution (60 mM final concentration). The resulting clear solution was then stirred for another 2–3 min, followed by the addition of 100 μL of 0.113 M $NaBH_4$ solution (prepared in 0.2 M NaOH solution). The reaction mixture was left stirring for ~3.5–4 h, and then growth was stopped when the fluorescence emission attained its highest value. The dispersion of NCs was concentrated to about 500 μL by applying one round of centrifugation using a membrane filtration device (with a cutoff M_W = 10 kDa). The NCs were washed one more time with DI water, concentrated to 500 μL, and then stored in the dark at 4 °C until further use.

Growth of gold-doped AgNCs (route 3)[45]

The growth of Au-doped Ag NCs was carried out under strong alkaline conditions, following the steps used to prepare the Cu and Ag-doped AuNCs described above (route 2).[45] Aqueous solutions of $AgNO_3$ and $HAuCl_4 \cdot 3H_2O$ (50 mM for both solutions) were added stepwise to the DHLA solution in water (4.5 mL). The total volume of precursor solution was fixed at 100 μL, while varying the molar fraction of $HAuCl_4 \cdot 3H_2O$ between 0 and 20% (see Table 3); the metal-to-DHLA ratio was maintained at 1 : 2 (this ratio was used in ref. 45). The growth was carried out for ~3.5–4 h, and then stopped when the photoemission attained its highest intensity. The dispersion of NCs was concentrated and washed with DI water before storage in the dark at 4 °C until further use. Additionally, we carried out growth of Au-doped Ag NCs in the presence of DHLA-PEG-OMe following the same steps above, except that no base was added, because the metal–ligand complex with PEGylated DHLA was readily soluble in water.

Spectroscopic characterization

UV-vis absorption measurements were carried out using a UV 2450 absorption spectrophotometer from Shimadzu (Columbia, MD), while fluorescence emission and excitation spectra were collected using a Fluorolog-3 spectrometer equipped with CCD and PMT detectors from Horiba Jobin Yvon Inc. (Edison, NJ). The fluorescence lifetime measurements were carried out using a time correlation single photon counting (TCSPC) system integrated into the same Fluorolog-3. We used a pulsed excitation signal at 440 nm with a repetition rate of 100 kHz, provided by NanoLED-440LH (100 ps, fwhm), while emission was collected with the same PMT detector as above. The fluorescence decay traces of AuNCs emission (limited to a narrow window centered at the peak of the PL spectrum) were analyzed using the TCSPC system and fitted to a mono-exponential decay function:

$$I(t) = I(0)e^{-\frac{t}{\tau}} \quad (1)$$

where t is time, $I(0)$ is the intensity at $t = 0$, and τ is the excited state lifetime.

The fluorescence quantum yield (QY) of the AuNCs was measured using Rhodamine 6G as a standard (QY_{ref} = 95% in ethanol) using the equation:

$$QY_{sample} = \frac{F_{sample}}{F_{ref}} \times \frac{A_{ref}}{A_{sample}} \times \frac{{n_{sample}}^2}{{n_{ref}}^2} \times QY_{ref}, \quad (2)$$

where F, A, and n are the measured fluorescence intensity (integrated area under the emission peak), the absorbance at the excitation wavelength, and the refractive index of the solvent, respectively. We used samples with absorbance values at the excitation wavelength smaller than 0.1, in order to minimize the effects of self-absorption.

ESI-TOF

(–) Electrospray mass spectrometry analysis was performed using a LCT Premier XE instrument (Waters Corporation). The instrument settings are summarized in Table 4.

X-ray photoelectron spectroscopy (XPS)

XPS spectra were collected using a PHI 5100 series instrument from PHI Inc. (Chanhassen, MN). The instrument is equipped with an un-monochromated Mg Kα source (1253.6 eV), and the pass energy of the analyzer was fixed at 89.45 eV. The photoelectron take-off angle was 45° relative to the sample surface. The binding energy (BE) scale of the system was calibrated using the energy of the orbitals $Au4f_{7/2}$ at 83.8 eV and $Ag3d_{5/2}$ at 368 eV. The samples were drop cast under flowing dry N_2 on freshly deposited graphite coated stubs. The spectra were collected by averaging over 15 sweeps using 0.05 eV steps and a 500 ms dwell time; a Shirley background was subtracted from all spectra before performing peak fitting to a Gaussian–Lorentzian function. The base pressure of the UHV analysis chamber was 6×10^{-10} mbar.

Table 3 Conditions used to grow Au-doped AgNCs following the protocol reported in ref. 45. Metal : ligand ratio = 1 : 2; [$NaBH_4$] = 100 μL (113 mM); [NaOH] = 150 μL (2 M); reaction time ~3–4 hours

$AgNO_3$ (50 mM)	100 μL	96 μL	92 μL	88 μL	84 μL	80 μL
$HAuCl_4 \cdot 3H_2O$ (50 mM)	—	4 μL	8 μL	12 μL	16 μL	20 μL

Table 4 Experimental conditions in the ESI-MS measurements

Solvent	$MeOH : H_2O$ = 1 : 1
Capillary voltage	−2200 V
Sample cone voltage	20 V
Desolvation temperature	200 °C
Source temperature	120 °C
Gas flow rate	200 L h^{-1}
Sample flow rate	20 μL min^{-1}

Gel-electrophoresis

Gel-electrophoresis was performed with a Sub-Cell GT Agarose Gel Electrophoresis System from BIO-RAD using 1% agarose medium (prepared in PBS buffer, pH 8) and a field strength of 10 V cm^{-1} for 15 minutes.

Phase transfer

In a scintillation vial, 100 μL of a concentrated aqueous dispersion of the NCs was first diluted to 500 μL with DI water. Then 500 μL of the organic solvent (chloroform, toluene or ethyl acetate) was added to the vial followed by addition of a small amount (~3–5 mg) of DDAB (a quarternary ammonium salt). After gentle shaking for few minutes, the NCs were readily transferred to the organic phase.

Results and discussion

Rationale

The approach we used to improve the properties of silver nanocrystals *via* doping with transition metal atoms builds on a combination of prior findings from our group and results described in the literature. (1) We have reported the use of one phase aqueous growth of Au and Ag nanoparticles and fluorescent nanoclusters starting from $HAuCl_4{\cdot}3H_2O$ or $AgNO_3$ mixed with LA or LA-PEG ligands and using $NaBH_4$ as the reducing agent.[22,37] In particular, we found that when a lipoic acid ligand (with no appended PEG) was used, the prepared nanoclusters tended to have low quantum yields (~3–4% maximum) for both core materials; higher yields (~12%) were measured from NCs grown in the presence of LA-PEG and LA-zwitterion ligands.[22,37] We also found that NCs made of pure Ag cores tended to exhibit limited long term PL stability, while LA-PEG-capped AuNCs with near IR emission had remarkable colloidal stability and maintained their emission for extended periods of time.[37] We were not able to carry out mass spectrometry measurements for any samples prepared with PEG-modified ligands, due to the polydispersity of PEG oligomers.[22,36,37,46] (2) A few recent reports have shown the benefits of growing metal alloy NCs, for which notable enhancement of the PL QY has been measured compared to pure core NCs. The groups of Jin and co-workers and Bakr and co-workers have reported the preparation of atomically precise NCs made of Ag-doped AuNCs or Au-doped AgNCs in an organic phase using small thiolate molecules. Both showed sizable enhancement of the measured PL (one to two orders of magnitude in each case). The pure materials prepared using either growth strategy exhibited very low fluorescence properties, nonetheless.[14,29] We thus reasoned that growing nanoclusters with mixed metal cores in the presence of LA- or DHLA-based ligands may yield materials with improved PL properties. In particular, we were intrigued by the possibility of growing bimetallic nanoclusters in an aqueous medium with improved photo-physical properties and enhanced PL.

We first tested the effects of doping Cu and Ag atoms into AuNCs prepared using the protocol described in our previous work (see Experimental section, Table 1).[37] The growth was carried out by reduction of a mixture of metal–dithiolate complexes, namely a mixture of Au/Ag or Au/Cu precursors complexed with lipoic acid (the oxidized form), in the presence of $NaBH_4$ under mild alkaline conditions (5 mM NaOH). However, we found that doping the AuNCs with either of those metals did not lead to any PL enhancement. Fig. 1 shows the UV-visible absorption and PL spectra of bimetallic Au nanoclusters prepared using various molar amounts of silver or copper precursors. The absence of a well-defined surface plasmon resonance peak around 520 nm in the absorption spectra indicates that the nanoclusters grown here are much smaller than conventional Au nanoparticles. Instead, a broad absorbance feature is measured in the spectra of the AuNC dispersions. (Note that such an absorption feature has been ascribed in previous studies to a combination of intraband (sp ← sp) and interband (sp ← d) transitions.[31]) The spectra also show that for Ag-doped NCs, the above broad peak (at ~500 nm for the AuNCs) decreased and a new feature appeared around 600 nm when the molar fraction of Ag was increased (see Fig. 1A). The red-shift in the absorbance feature has been attributed to a decrease in the HOMO–LUMO gap for Au_{25}NCs upon doping with a few Ag atoms.[26,45] The PL increased slightly at a Ag molar fraction of 5%, but continuously decreased for higher fractions (see Fig. 1B). Conversely, when a Cu precursor was used, the absorption feature at 500 nm disappeared at a Cu molar fraction exceeding 10% (see Fig. 1C). Similarly, the PL emission substantially decreased with increasing Cu (see Fig. 1D). This implies that doping transition metals such as Cu and Ag into AuNCs *via* this route does not improve the photo-physical properties of the resulting materials.

We then tested the effectiveness of growing Ag- and Cu-doped AuNCs under strong alkaline conditions as reported by Xie and co-workers, which they utilized to prepare monothiolate-protected Au_{25} and $Au_{25-x}Ag_x$ NCs.[45,47] The authors have suggested that the use of a base can provide better control over the growth rate of AuNCs using a variety of thiolate ligands, thus improving the homogeneity of the materials.[47] We carried out the growth of Au/Ag and Au/Cu nanoclusters under strong alkaline conditions using bidentate DHLA as the capping ligand. However, this growth protocol also yielded Ag- and Cu-doped AuNCs with marginal PL enhancement for all molar fractions tested over the range 0–50%; albeit a small increase was measured for Ag-doped samples. The absorption spectra were overall featureless with a sizable increase that was limited to the UV region. The absorption and emission spectra are provided in the ESI,† Fig. S1.

However, we found that when growth under highly alkaline conditions was applied to the doping of Au atoms into AgNCs, it yielded bimetallic NCs with substantially better photophysical properties. Characterization and optimization of those bimetallic nanoclusters will be described below. We should note that the nanoclusters grown in the presence of monothoiolate ligands described in Xie's work exhibit variations in the UV-visible absorption spectra depending on the level of doping, but the resulting materials were essentially non-fluorescent.[45,47]

Growth and optical characterization of bimetallic Au-doped AgNCs

$AgNO_3$ and $HAuCl_4{\cdot}3H_2O$ were first mixed with DHLA (the reduced ligand) to allow formation of the Au- and Ag-ligand complexes (precursors). Reduction of the metal–ligand complexes coupled

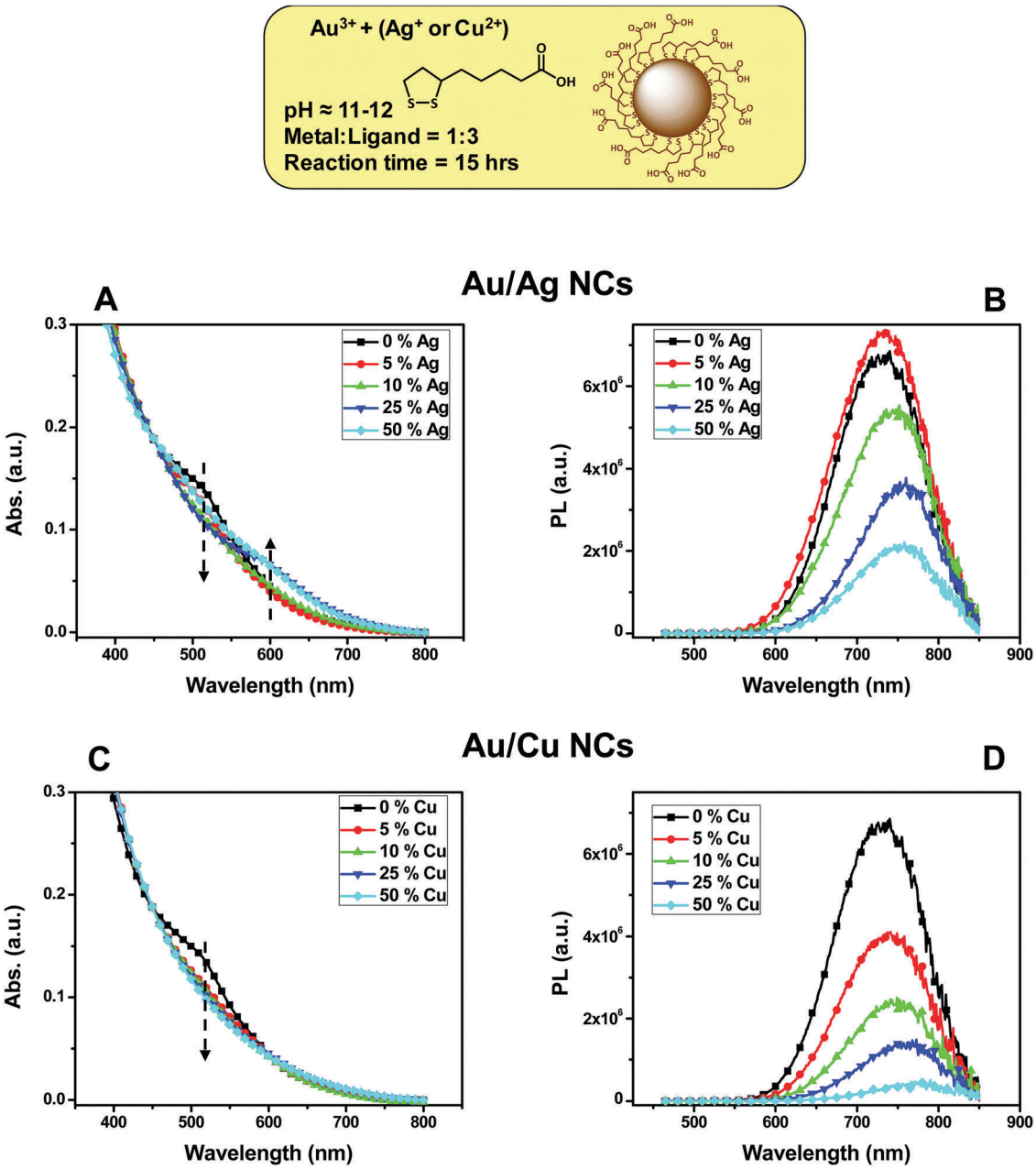

Fig. 1 Photophysical characteristics of the Ag- and Cu-doped AuNCs prepared following the protocol detailed in ref. 37. (Top) Schematic representation of the growth reaction used. (A and B) UV-visible absorption and PL spectra collected from Ag-doped AuNCs. (C and D) UV-visible absorption and PL spectra collected from Cu-doped AuNCs.

with growth of the nanocluster material was carried out using sodium borohydride, and the growth was monitored by periodically collecting the optical absorption and emission spectra until the PL emission reached saturation (after approx. 3.5–4 hours). Fig. 2 shows a few representative spectra of the Au-doped AgNCs, prepared using Au molar fractions ranging from 4 to 20%, together with those collected from the pure AgNCs (panels B and C). The full set of collected spectra are provided in the ESI,† (Fig. S2). We first note that the resolved features in the absorption and excitation spectra are overall maintained throughout the range of molar fractions used. Data also show that there is a blue shift in the absorption features, namely, the peak at 495 nm shifted to 475 nm, while that at 422 shifted to 405 nm, when the molar amount of Au-precursor was increased (Fig. 2B). These changes are reflected in the excitation spectra shown in Fig. 2D. The largest enhancement of the PL intensity, which reached a 6-fold increase compared to pure AgNCs, occurred at a Au molar fraction of 8%, but decreased again when higher amounts of gold precursor were used. There is a small red-shift in the PL peak location (from 680 to 688 nm) measured for the doped nanoclusters. We also compared the time-resolved fluorescence profiles collected from dispersions of pure AgNCs and AgAuNCs

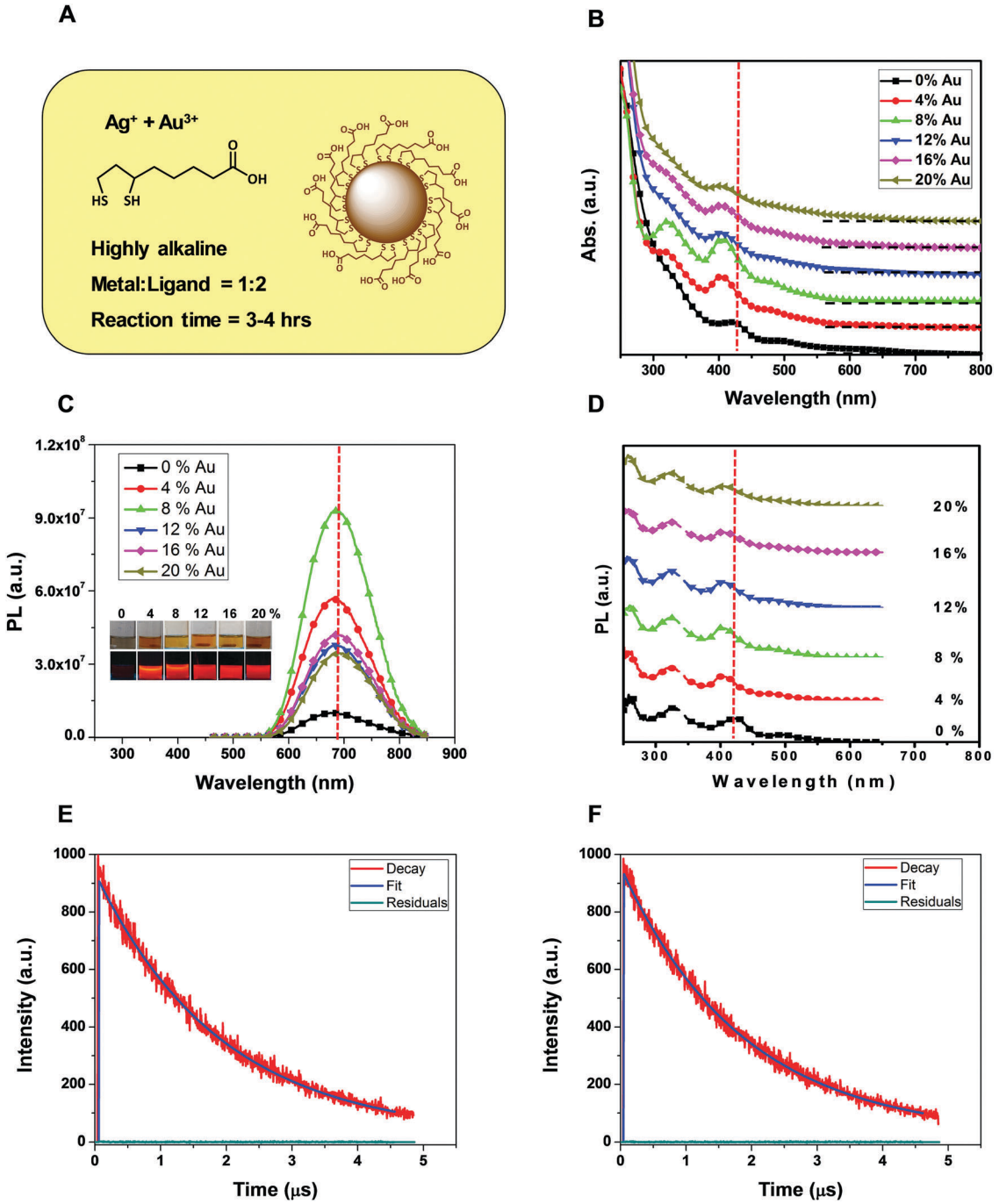

Fig. 2 (A) Schematic representation of the growth reaction used. (B and C) UV-vis absorption and PL emission spectra collected from AgNCs and Au-doped AgNCs prepared using the method introduced in ref. 40. The molar fractions of gold precursors were varied from 0 to 20%; the growth reaction time was ~3.5 hours. The PL spectra were collected using 450 nm excitation and normalized with respect to absorbance at 450 nm. Inset in panel C shows images of the NC dispersions under room light and UV light exposure. (D) The corresponding PL excitation spectra collected using a detection wavelength at the PL peak. (E and F) Time-resolved PL profiles collected from dispersions of AgNCs (undoped, E) and AuAgNCs prepared using 8% gold precursor (F). The profiles were fit to a single exponential decay function (eqn (1)).

(at 8% Au), and found that that both profiles can be fitted using a mono-exponential decay function (eqn (1)), see Fig. 2E and F. The average fluorescence lifetimes are provided in Table 5. Rather long life-times of 1.86 μs and 1.91 μs were measured for the Ag_{29} and $AuAg_{28}$ nanoclusters, respectively. Similar long lifetimes have also been reported for other red and near-IR emitting nanoclusters.[25,48] It has been suggested that such long fluorescence lifetimes are mainly due to a metal-to-ligand charge transfer process.[25]

Next, we explored the growth of Au-doped AgNCs using poly(ethylene glycol) (PEG)-substituted DHLA (DHLA-PEG) ligands, but limited the Au doping to a molar fraction of ~8%. This is the

Table 5 Excited State lifetimes of Ag_{29} and $AuAg_{28}$ NCs in water. Samples were excited at 440 nm and the PL was collected at the peak value

	τ (μs)	χ^2
Ag_{29}	1.86 ± 0.02	1.06
$AuAg_{28}$	1.91 ± 0.02	1.02

value that produced the largest enhancement of the PL signal measured for the DHLA-capped NCs discussed above (Fig. 2C). Appending a short polyethylene glycol block onto LA (and DHLA) has been shown to expand the solubility and to drastically improve the colloidal stability and biocompatibility of a variety of plasmonic and semi-conductor nanocrystals.[37,43,49] We followed the same protocol described above, albeit with one modification. No excess base was added prior to the reduction of the metal–ligand complex by sodium borohydride, as the metal–ligand complex was already soluble in water (unlike the metal–DHLA complex). Additionally, we found that the addition of base to the growth reaction in the presence of DHLA-PEG significantly slowed the growth kinetics and weakened the PL intensity (see ESI,† Fig. S3). Fig. 3A and B show a side-by-side comparison between the absorption and PL properties of AgNCs and AgAuNCs grown in the presence of DHLA-PEG-OCH_3 and DHLA. The time-progression of the spectra collected during the growth of the AuAgNCs (8% gold) is provided in the ESI,† (Fig. S3, panels A and B). Data indicate that the PL intensity of DHLA-PEG-OCH_3 capped AgNCs is comparable to that of DHLA capped AgNCs. Furthermore, doping of Au into AgNCs leads to a ~5–6-fold enhancement of the PL combined with a slight blue-shift of the absorption peaks. This indicates that the effects of doping on the absorption and PL spectra are comparable when the reduced form of either set of ligands is used (see Fig. 3A and B). These findings contrast with earlier data reported by our group where we showed that the growth of pure AgNCs *via* borohydride reduction using LA-PEG-OCH_3 (the oxidized form) yielded a material significantly more fluorescent than that grown using the oxidized LA.[22] To develop a more comprehensive comparison between the effects of doping and the nature of the ligand, we complemented our experiments by testing the effects of modifying the nature of the thiolated ligands, LA- *vs.* DHLA-modified PEG ligands, on the growth of pure AgNCs. We evaluated the fluorescence properties of AgNCs grown using LA-PEG-OCH_3 instead of DHLA-PEG-OCH_3 as above to allow a direct comparison between the Ag-based NCs prepared in this study using the reduced form and those grown using the oxidized form of the ligand, for which a higher PL emission (PL QY of ~12%) was measured for AgNCs, as detailed in ref. 22 and 37. The data in Fig. 3C and D show that the PL intensity of AgNCs prepared using LA-PEG-OCH_3 yielded higher PL emission than those grown using the reduced DHLA-PEG-OCH_3 in agreement with our previous findings.[22] Furthermore, we found that when Au-doping of AgNCs was carried out using the oxidized ligands, a rather small enhancement of the PL was measured (see Fig. 3E and F). These findings clearly prove that the quality of NCs and the effects of Au-doping of AgNCs grown by borohydride reduction in the presence of LA-based ligands depend on the nature of the coordinating group (disulfide *vs.* dithiol). When the oxidized form is used to grow the NCs, it yields materials with high QY, but a rather small improvement is brought about by Au-doping (a ~20–25% enhancement of the PL). Conversely, when the reduced form of the ligand is used, growth yields AgNCs with rather modest PL emission, but the effects of Au-doping are much more pronounced (~5–6 times). This result is likely due to a difference in the metal-to-ligand complexation and thus the nature of the precursors involved in the NC growth.

Mass and size characterization

Mass spectrometry. The stoichiometry of AgNCs grown using DHLA has been recently investigated by Antoine and coworkers using mass spectrometry, who reported that the composition of the prepared nanoclusters was $Ag_{29}(DHLA)_{12}$.[36] We used (–) ESI-MS to characterize our AgNCs and Au-doped AgNCs and limited our measurements to DHLA-capped NCs; characterization of DHLA-PEG-capped nanoclusters is complicated by the nature and inherent polydispersity of the PEG moieties.[22] Fig. 4 shows the ESI spectra collected from NC dispersions prepared using either pure Ag, or a mixture containing 8% Au-precursor. Additional (–) ESI mass spectra collected from samples grown with Au doping ranging from 0 to 20% are provided in the ESI,† Fig. S4. The mass spectra of both sets of NCs show peaks in two regions: one set at ~1100–1200 amu corresponding to species with a net negative charge of −5 and the other at ~1400–1500 amu corresponding to species with a net negative charge of −4 (see Fig. 4). The two sets of peaks at 1120 amu and at 1400 amu (insets) correspond to nanoclusters with a stoichiometry of $Ag_{29}(DHLA)_{12}$ having charges of −5 and −4, respectively. Each of the two sets contains multiple peaks that only differ by ~4.4 and ~5.5 units, which can be ascribed to the formation of sodium adducts ([Na–H]/5 = 4.4 and [Na–H]/4 = 5.5). The peaks of the gold-doped NCs (Ag_xAu_yNCs) are shifted by ~18 and ~22 units relative to those measured for the pure AgNCs (compare panels A and B in Fig. 4). These features correspond to the presence of a single gold atom with a difference of 89/5 and 89/4, respectively; 89 is the difference between the atomic masses of gold and silver. The ESI-MS data indicate that one dominant stoichiometry of the bimetallic NCs was grown, $AuAg_{28}$ NCs; other combinations may be present but at very small concentrations.

X-ray photoelectron spectroscopy

X-ray photoelectron spectroscopy (XPS) measurements were carried out to analyze the valence states of silver and gold atoms in the AgNCs and AgAuNCs grown using DHLA ligands. Fig. 5, panels A and B show the XPS spectra focusing on the energy region associated with the Ag3d peaks for AgNCs and Au-doped AgNCs. The $Ag3d_{5/2}$ peaks was observed at a higher energy (at ~369–369.5 eV) compared to the Ag(0) film (measured at ~368 eV, represented by the vertical dashed line). This positive energy shift can be attributed to surface coordinated thiolates, as measured for Ag evaporated on a poly(*p*-phenylene sulfide) film and for Ag_2S.[50] Fig. 5, panel C shows the XPS spectrum from the bimetallic AgAu nanoclusters focusing on the Au4f region. The $Au4f_{7/2}$ peak is observed at ~85.7 eV, which is very close to that anticipated for AuNCs and seen for Au(I) complexes (86.1 eV).[31,51]

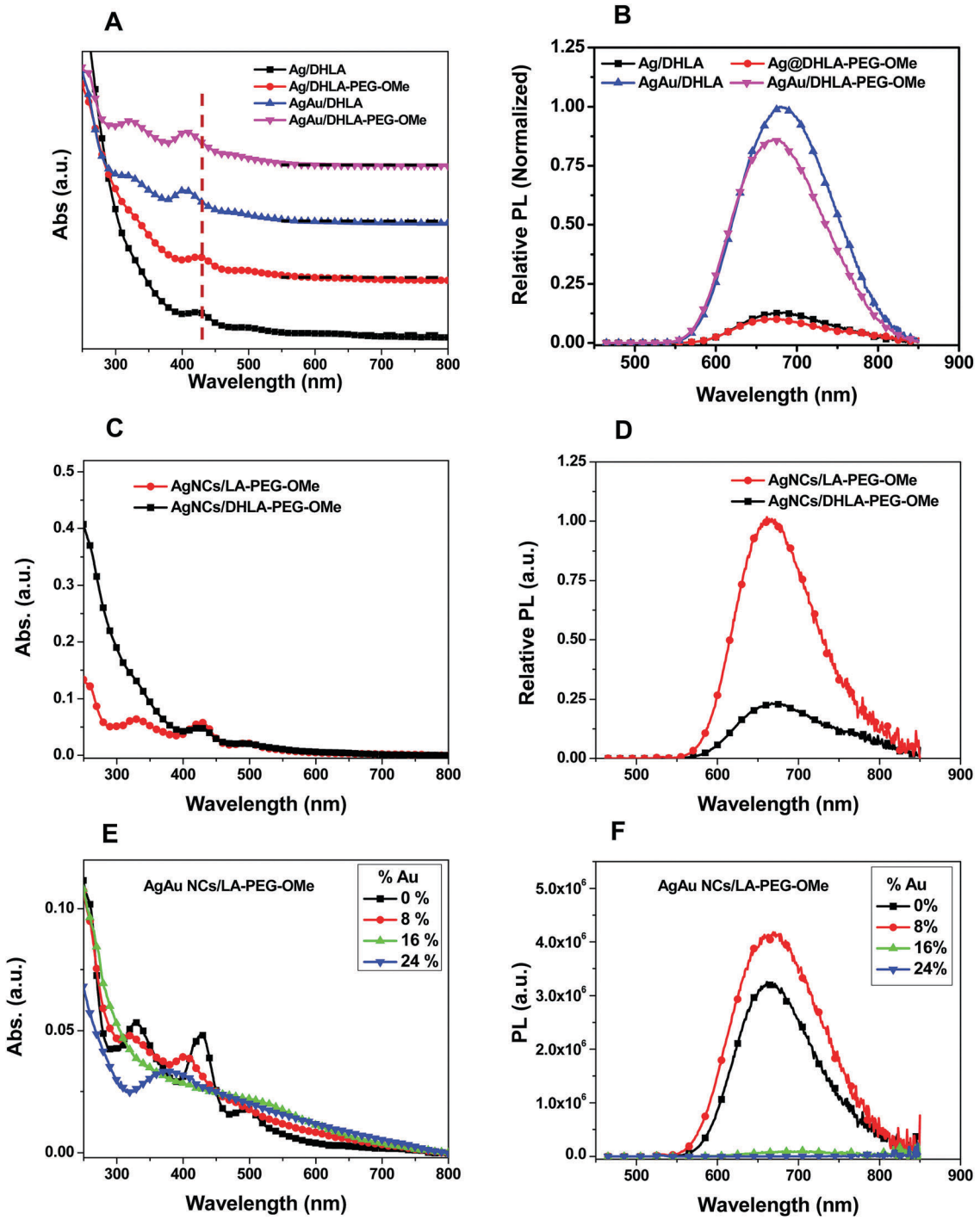

Fig. 3 (A and B) Side-by-side comparison of the absorption and PL spectra collected from Ag and Au-doped AgNCs, grown in the presence of the reduced ligands, DHLA and DHLA-PEG-OCH_3. The spectra for DHLA capped NCs are shown for comparison. (C and D) Absorption and emission spectra collected from AgNCs grown in the presence of the oxidized LA-PEG-OCH_3, or the reduced DHLA-PEG-OCH_3, following the protocol described in ref. 24. (E and F) Absorption and PL spectra of AgNCs and Au-doped AgNCs prepared using LA-PEG-OCH_3, as done in ref. 22. The effects of doping on the PL were marginal.

Hydrodynamic size measurement. We have also applied diffusion ordered NMR spectroscopy (DOSY) to estimate the diffusion coefficients and hydrodynamic sizes of the pure AgNCs and Au-doped AgNCs. This technique has emerged as a very useful analytical tool to estimate the hydrodynamic sizes of ultra-small nanoparticles.[52] The diffusion coefficient can be combined with the Stokes–Einstein equation ($R_H = k_B T/6\pi\eta D$, where k_B is the Boltzmann constant, T is the temperature, and η is the solvent viscosity) to obtain an estimate for the hydrodynamic size, R_H. This approach has been recently utilized to

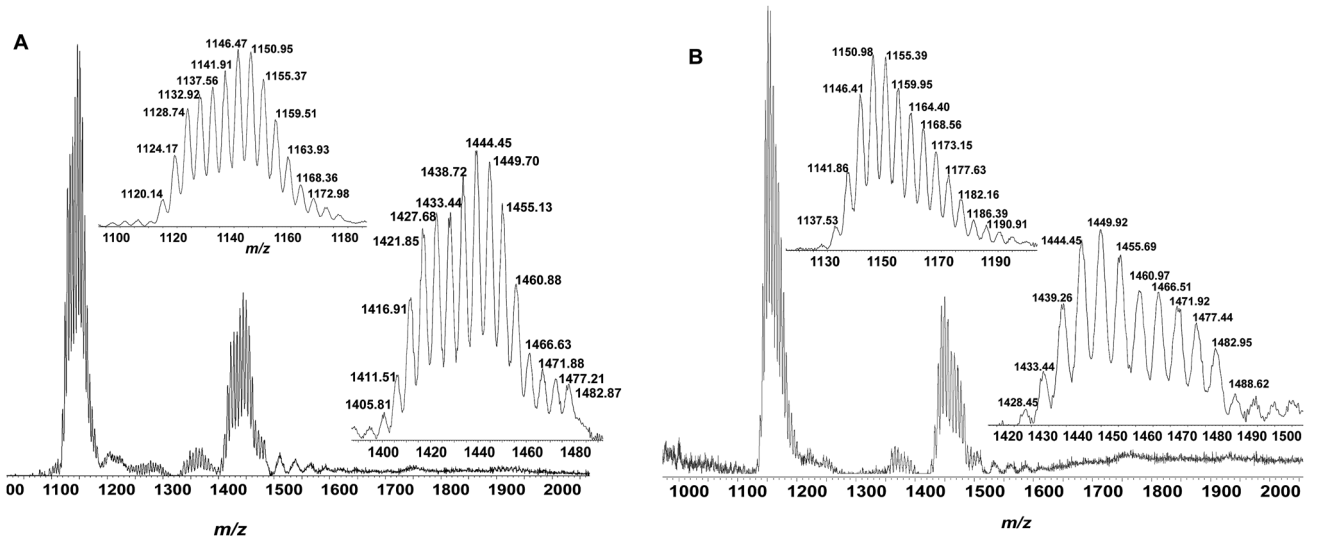

Fig. 4 (A) ESI-MS of Ag_{29} and (B) $Ag_{28}Au$ NCs. The peaks at 1100–1200 amu correspond to −5 charged species and those at 1400–1500 amu correspond to −4 charged species. Enlarged views of each of the segments are shown for both species.

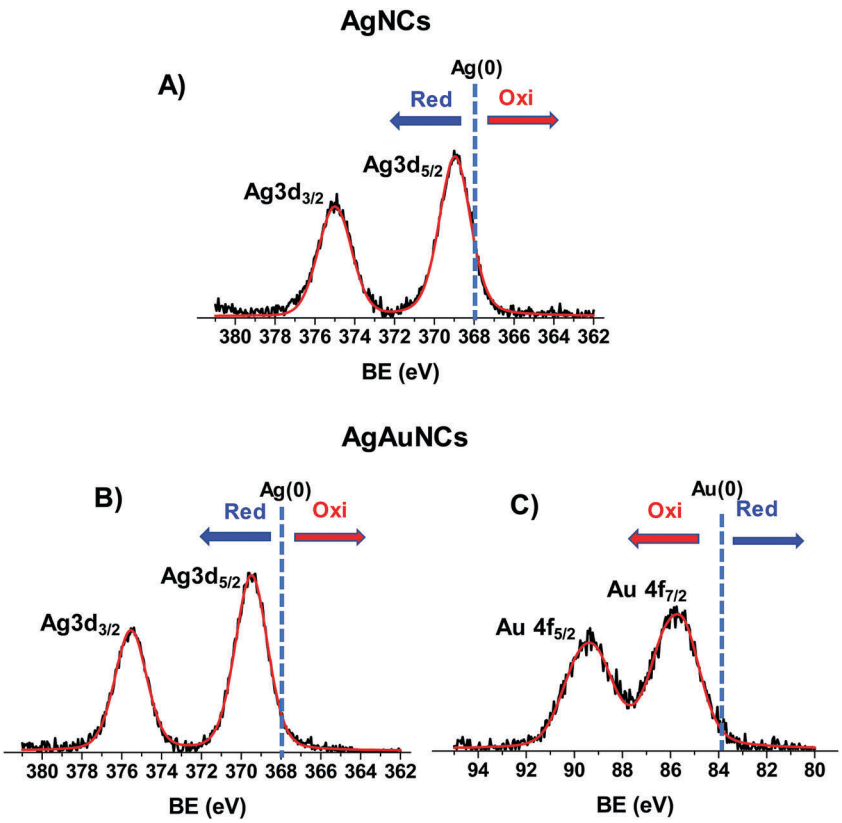

Fig. 5 XPS spectra for (A) Ag3d peaks in AgNCs (B) Ag3d peaks in AgAuNCs and (C) Au4f peaks in AgAuNCs. The positions corresponding to Ag(0) and Au(0) are indiciatd with dashed lines.

extract R_H values for AuNCs.[51,53] Fig. 6 shows the DOSY plots of AgNCs and 8% Au-doped AgNCs grown using DHLA or DHLA-PEG-OCH_3 ligands. The average diffusion coefficients and the calculated hydrodynamic radii of Ag_{29} and $AuAg_{28}$ NCs using DHLA and DHLA-PEG-OCH_3 ligands are compiled in Table 6. Data indicate that similar diffusion coefficients, D, or hydrodynamic sizes, R_H, are measured for the doped and undoped NCs; when PEGylated ligands are used to grow the nanoclusters, the change in D and R_H are commensurate with an overall increase in the NC dimensions (accounting for contributions

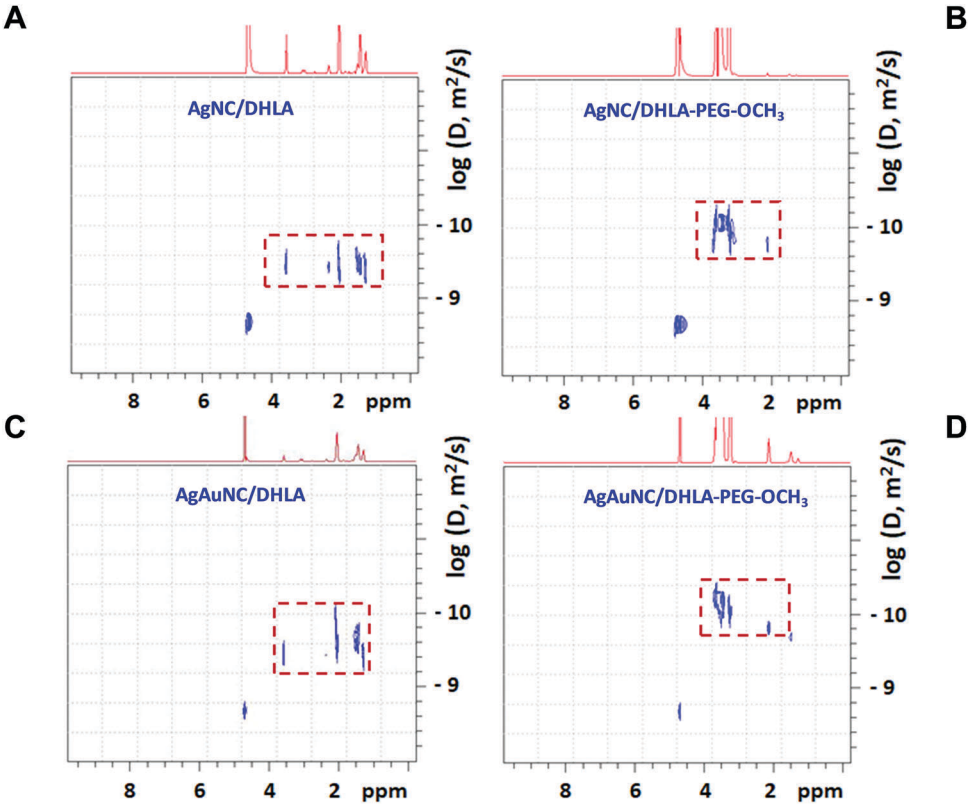

Fig. 6 DOSY plots of: (A) DHLA capped Ag_{29} NCs, (B) DHLA-PEG-OCH_3 capped Ag_{29} NCs, (C) DHLA capped Au-doped (8%) Ag_{29} NCs and (D) DHLA-PEG-OCH_3 capped Au-doped (8%) Ag_{29} NCs. Diffusion coefficients and hydrodynamic radii of Ag and Au-doped Ag NCs obtained from DOSY NMR are listed in Table 6. The data were collected in D_2O at room temperature, $D(H_2O) = 1.76 \times 10^{-9}$ m^2 s^{-1}.

Table 6 Diffusion coefficients and hydrodynamic radii measured using DOSY NMR for DHLA and DHLA-PEG-OCH_3 capped nanoclusters in water

	$10^{10} \times D$ (m^2s^{-1})	R_H (nm)
Ag_{29}/DHLA	3.55 ± 0.75	0.63 ± 0.15
$AuAg_{28}$/DHLA	3.46 ± 0.74	0.65 ± 0.13
Ag_{29}/DHLA-PEG-OH_3	1.28 ± 0.58	2.10 ± 1.10
$AuAg_{28}$/DHLA-PEG-OH_3	1.14 ± 0.52	2.24 ± 1.02

of the inorganic core and organic shell). They also confirm that the Au substitution had a negligible effect on the overall dimensions of the ligand-capped NCs.

Phase transfer to organic solvents

Although several studies have focused on the phase transfer of hydrophobic NCs to aqueous media, often relying on ligand exchange or encapsulation within amphiphilic micelles, the reverse process may be informative even though it has been less explored. One strategy to achieve this goal exploits the effects of electrostatic interactions to promote complexation between ligands with distinctly different natures and affinities on the surface of the NCs and facilitate phase transfer; such a strategy depends on the net charge density present on the surface of the starting NCs.[9] Recently, Ramakrishna and coworkers used this strategy to phase transfer glutathione stabilized gold NCs from water to an organic phase, which ultimately led to enhanced photoluminescence of the otherwise weakly emitting native NCs in the aqueous phase.[54] We applied this approach to our DHLA-capped NCs and found that introducing the phase transfer catalyst DDAB readily promoted the transfer of the as-prepared, DHLA-capped $AuAg_{28}$ NCs to organic solvents. The polar carboxylic acid groups of DHLA readily interacted with DDAB as schematically depicted in Fig. 7, altering the compatibility of the NCs. Additionally, we found that the optical absorption features, as well as the PL spectra, are preserved following transfer to organic media; albeit a slight enhancement (~20–25%) of the PL emission was measured. Phase transfer of these nanoclusters to organic media can be beneficial for long-term storage as well as for their use in potential applications. We should note that the NCs grown using DHLA-PEG-OCH_3 ligands are readily dispersible in different organic solvents, due to the amphiphilic nature of ethylene glycols, a result consistent with our previous findings.[37]

Colloidal stability

The as prepared DHLA-capped AgNCs and AuAgNCs are stable under basic conditions (pH > 7). However, the fluorescence of these NCs rapidly decreases when dispersed in acidic buffer. In particular, at pH ≤ 5, a pronounced loss in the fluorescence emission was measured, though the UV-vis absorption features were fully preserved (see ESI,† Fig. S5). This observation suggests that the surface atoms involved in the coordination interactions with the ligands, combined with potential changes in the ligand

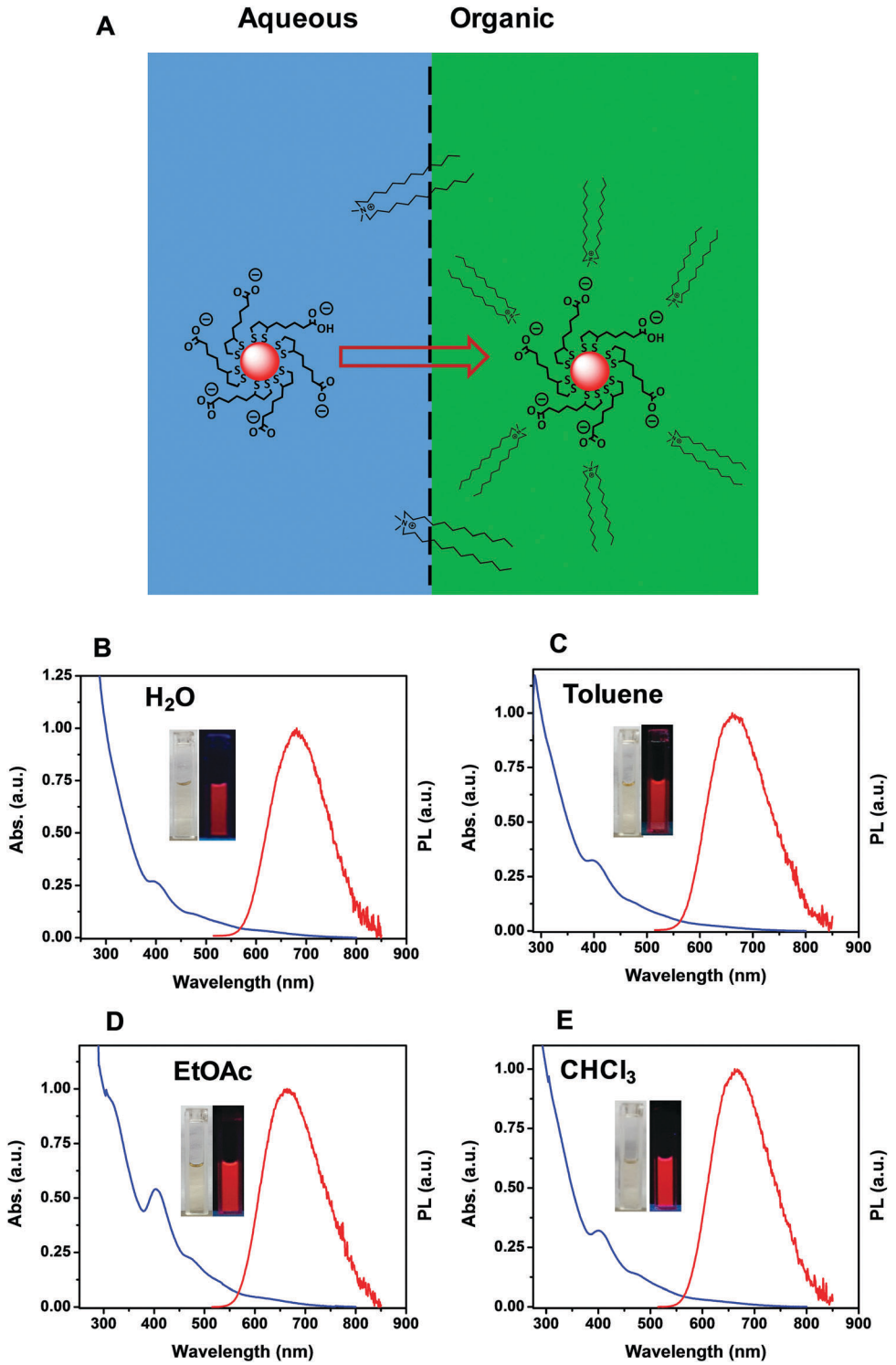

Fig. 7 (A) Schematic representation of the phase transfer of $AuAg_{28}$ NCs from an aqueous to organic phase. (Right) UV-visible absorption and PL emission spectra of the NCs in (B) water, (C) toluene, (D) ethyl acetate and (E) chloroforom. The images shown in the insets are of the various dispersions under room light and UV light exposure.

structure, play an important role in controlling the emission and stability of these NCs. Earlier reports have suggested that the pH of the medium can affect the binding of the thiol group to AgNC surfaces and significantly alter their optical properties.[35] The pK_a of the –COOH and –SH groups in the DHLA molecule are ~4.85 and 10.7 respectively.[55] Thus, under strongly basic conditions (pH > 11), the combined deprotonation of the thiol and COOH groups promotes strong bidentate interactions with the surfaces along with steric stabilization of the NCs, yielding stronger and more stable emission. At pH < 4.85, the protonation of the

carboxylic acid group and likely one of the thiol groups reduces the surface passivation of the NCs and alters their steric stability, ultimately promoting slow aggregation and a loss of fluorescence. The stability of the AuAgNCs in acidic pH was improved when PEG (polyethylene glycol) appended DHLA was used, an expected outcome given the broader solubility range allowed by PEG moieties. PEGylation of the NC surfaces promoted colloidal stability in a phosphate buffer over the pH range 3–13 (see ESI,† Fig. S6). This constitutes an improvement compared to NCs with pure Ag cores as described in ref. 22. We should also note that the NCs are sensitive to UV light exposure, where a nearly complete loss in PL was measured after 30 minutes (ESI,† Fig. S7). The effects of UV irradiation on the photoemission of AgNCs have been reported by Sanz-Medel and coworkers, who suggested that photo-oxidation of the AgNCs and formation of larger size nanoparticles takes place.[56] Nonetheless, we have found that if dried and stored under inert conditions (nitrogen or argon), the NCs can maintain their integrity and fluorescence properties for at least 6 months of storage.

Surface functionalization

The route used in this study allows easy introduction of specific functional groups on the NCs *in situ* during nanocluster growth, by simply using a ligand mixture containing a small fraction of DHLA-PEG-R during the growth.[37] The gel electrophoresis image shown in Fig. 8 indicates that growth carried out in the presence of PEG-amine or PEG-COOH yields NCs with mobility shifts commensurate with the nature of the group: amine-NCs migrate towards the cathode and COOH-NCs migrate towards the anode, while OCH_3-NCs essentially exhibit no mobility shift. This result implies that our growth route, combined with the use of mixed ligands, can permit the introduction of other reactive groups provided that they are not affected/altered by sodium borohydride. A slight decrease in the PL intensity was measured for –COOH and $-NH_2$ functionalized NCs (~10% and ~30% respectively), compared to $-OCH_3$ terminated NCs.

Discussion

We would like to discuss our results in comparison with previous findings reported by our group and within the general concept of using transition metal doping of Au and Ag nanoclusters as a means of improving the photo-physical properties of such materials. Table 7 shows a side-by-side comparison of the properties of the NCs with single metal and bimetallic cores, prepared using aqueous growth in the presence of the various lipoic acid-based ligands.[22,37] Clearly the effects of doping are most pronounced when using the reduced forms of the ligands (DHLA and DHLA-PEG). However, such an increase is also strongly dependent on the starting pure NCs. Indeed, our data show that growth in the presence of the oxidized form of the ligands yields relatively high PL for the pure cores, but the enhancement promoted by doping is marginal. In contrast, when the reduced form is used, rather modest PL is measured for the pure core materials and doping increased the PL by ~5–6 times. The effects of NaOH are pronounced for DHLA, where they play an essential role in promoting ligand solubility, but PEGylation eliminates the need for alkaline conditions.

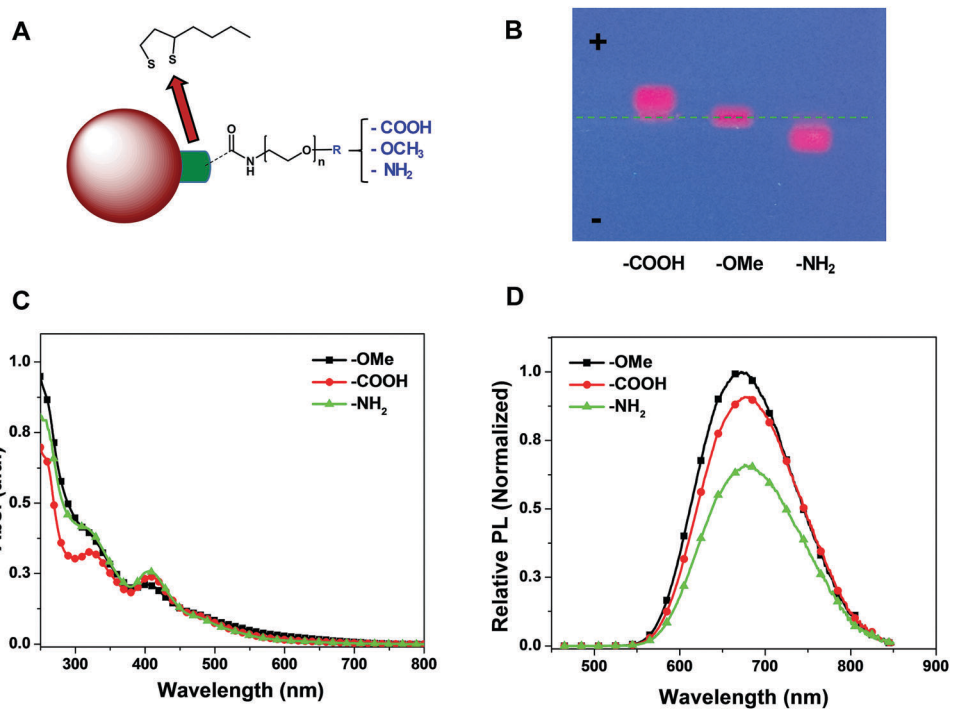

Fig. 8 (A) Functionalization of the bimetallic NCs using ligands terminated with $-COOH$ and $-NH_2$ groups. (B) Gel electrophoresis image showing the change in the mobility band as a function of the terminal group used. Band designations: OMe (100% DHLA-PEG-OCH_3), –COOH (10% DHLA-PEG–COOH), and $-NH_2$ (30% DHLA-PEG-NH_2). The absorption and PL spectra of the three sets of functionalized NCs are shown in panels C and D.

Table 7 Side-by-side comparison of the growth conditions used to prepare Ag, Au and Au-doped Ag nanoclusters along with the measured PL quantum yields

	AgNC/ LA-PEG-OMe[a]	AgAuNC/ LA-PEG-OMe	AuNC/ LA-PEG-OMe[b]	AgNC DHLA	AgAuNC/ DHLA	AgNC/LA	AgAuNC/LA	AgNC/ DHLA-PEG-OMe	AgAuNC/ DHLA-PEG-OMe	AgAuNC/ DHLA-PEG-OMe
[Metal precursor]	0.05 mM	0.05 mM	0.5 mM	1 mM	1 mM	1 mM	1 mM	1 mM	1 mM	1 mM
[Ligand]	0.05 mM to 0.5 mM	0.05 mM to 0.5 mM	1.5 mM	2 mM	2 mM	2 mM	2 mM	2 mM	2 mM	2 mM
[$NaBH_4$]	1 mM	1 mM	1 mM	1 mM	1 mM	1 mM	1 mM	1 mM	1 mM	1 mM
[NaOH]	No base	No base	5 mM	60 mM	60 mM	60 mM	60 mM	4–5 mM	4–5 mM	60 mM
Effects on PL	QY ~ 12	QY ~ 15%	QY ~ 12–14%	QY ~ 3%	QY ~ 20%	Poorly emitting (QY <1%)	Minor increase	3%	18%	Slow growth

[a] NCs prepared following the protocol reported in ref. 22. [b] NCs prepared following the protocol reported in ref. 37.

Our proposed NC stoichiometry, $Ag_{29}(DHLA)_{12}$, which is in agreement with independent findings reported by Antoine and co-workers, was made possible only in the absence of PEG moieties.[36] This is also in agreement with reports of Bakr and co-workers who used slightly different growth conditions, namely an organic phase and a mixture of 1,3 benzenedithiol and phosphine ligands. They too identified NCs with 29 core atoms, *i.e.*, $[Ag_{29-x}Au_x(BDT)_{12}(TPP)_4$, x = 1–5, BDT = 1,3 benzenedithiol (BDT) and TPP = triphenylphosphine] in the organic phase. They reported a PL increase commensurate with the molar fraction of gold precursor used up to 24%, a result that contrasts with our finding where the beneficial effects of Au doping were limited to a low molar fraction of ~8%.[29] Their X-ray diffraction data collected from Au-doped Ag NCs suggested that clusters with single Au atom doping, *i.e.* $Ag_{28}Au(TPP)_4(BDT)_{12}$, could be identified, regardless of the amount of gold precursor used; their mass spectrometry data showed higher level of doping, nevertheless. The enhancement of the ensemble PL is also accompanied by a slight increase in the excited state lifetime. In addition to experimental data, PL enhancement promoted by transition metal doping has been discussed conceptually. Time-dependent density functional calculations on these clusters were carried out by Muniz-Miranda and co-workers and their findings indicated that the origin of this PL enhancement lies in the nature of the first excited states.[57] Upon doping, the low energy "dark" states are shifted to high energy "radiative" states. Similar conclusions were drawn by Hakkinen's group using DFT to model the optical properties of the $Ag_{29-x}Au_x$ nanoclusters discussed above.[29,58] In general, these studies suggest that perturbation of the electronic relaxation and the dynamics of the doped clusters is induced by the dopant atoms. We should note that the increase in the PL quantum yield and the lifetime of doped silver relative to the pure Ag_{29} NC is still not clearly understood. In their study, Bakr and coworkers proposed the formation of a new-excited singlet state with varying degrees of charge transfer between the ligand and the metal atoms.[29] When compared to the doping protocol reported by Xie and co-workers, we found that aqueous growth using DHLA and strong alkaline conditions yielded homogeneous nanoclusters with emission that can be strongly enhanced by Au-doping. Thus, our results support and complement the results reported by Xie and co-workers. Our findings are overall in agreement with recent data on bimetallic nanoclusters made of Au cores doped with a range of transition metals (Ag, Pt, Cu, Zn, *etc.*) starting with the oxidized LA-PEG ligands reported by Oh and co-workers.[59] We hypothesize that the rather low level of Au doping into the Ag_{29} NCs may be due to the relatively short growth period of 3.5–4 hours (the time required for the maximum PL emission to occur) combined with the thermodynamic stability of the "monogold" doped AgNCs.

Conclusion

We have described a simple protocol, using borohydride reduction in the presence of lipoic acid-derivatives, to grow magic size nanoclusters of silver and Au-doped silver cores in water solutions. We showed that gold doping achieved *via* co-reduction of Au and

Ag precursors, in the presence of the reduced form of the ligand and under alkaline conditions, yielded a ~5–6 fold enhancement of the PL quantum yield, compared to the pure Ag core material. A small increase in the average fluorescence lifetime upon doping was also measured, which suggests the appearance of new electronic states with higher radiative recombination rates. The effects of doping were equally reflected in the absorption profiles collected from these materials, where changes in the spectral features were measured when an increase in the molar fraction of the Au precursor was introduced during growth. The composition of both sets of NCs was characterized by mass spectrometry and magic sizes of $Ag_{29}(DHLA)_{12}$ and $Ag_{28}Au(DHLA)_{12}$ have been identified. We found that the introduction of didodecyldimethylammonium bromide (a quarternary ammonium salt) can promote the phase transfer of aqueous grown DHLA-capped NCs to organic media, which could improve the stability and shelf-life of these nanoclusters.

Similar effects of doping were obtained when DHLA-PEG-OCH_3 was used to grow the NCs. Data indicate that the nature of the coordinating group, LA *vs.* DHLA, affects the PL properties of the pure NCs and the level of Au-induced PL enhancement. Additionally, our growth route allows *in situ* functionalization of the NCs with groups such as $-NH_2$ and –COOH. The stability and dispersibility of these materials in both aqueous and organic media is promising for their potential applications in optical sensing and imaging. The strong absorption in the visible spectrum accompanied by a long fluorescence lifetime also makes them suitable for use in light harvesting devices.

Conflicts of interest

There are no conflicts to declare.

Acknowledgements

The authors acknowledge FSU and the National Science Foundation for financial support (NSF-CHE #1508501). We thank the National High Magnetic Field Laboratory (NHMFL) for providing the ESI-MS facility, and Tingting Jiang (FSU, NHMFL) for the helpful discussions.

References

1 J. Xie, Y. Zheng and J. Y. Ying, Protein-Directed Synthesis of Highly Fluorescent Gold Nanoclusters, *J. Am. Chem. Soc.*, 2009, **131**, 888–889.
2 V. Bonacic-Koutecky, A. Kulesza, L. Gell, R. Mitric, R. Antoine, F. Bertorelle, R. Hamouda, D. Rayane, M. Broyer, T. Tabarin and P. Dugourd, Silver cluster-biomolecule hybrids: from basics towards sensors, *Phys. Chem. Chem. Phys.*, 2012, **14**, 9282–9290.
3 S. Choi, R. M. Dickson and J. Yu, Developing luminescent silver nanodots for biological applications, *Chem. Soc. Rev.*, 2012, **41**, 1867–1891.
4 Y. Lu and W. Chen, Size effect of silver nanoclusters on their catalytic activity for oxygen electro-reduction, *J. Power Sources*, 2012, **197**, 107–110.
5 S. Ghosh, U. Anand and S. Mukherjee, Luminescent Silver Nanoclusters Acting as a Label-Free Photoswitch in Metal Ion Sensing, *Anal. Chem.*, 2014, **86**, 3188–3194.
6 S. M. Copp, D. E. Schultz, S. Swasey and E. G. Gwinn, Atomically Precise Arrays of Fluorescent Silver Clusters: A Modular Approach for Metal Cluster Photonics on DNA Nanostructures, *ACS Nano*, 2015, **9**, 2303–2310.
7 R. Jin, C. Zeng, M. Zhou and Y. Chen, Atomically Precise Colloidal Metal Nanoclusters and Nanoparticles: Fundamentals and Opportunities, *Chem. Rev.*, 2016, **116**, 10346–10413.
8 W. A. de Heer, The physics of simple metal clusters: experimental aspects and simple models, *Rev. Mod. Phys.*, 1993, **65**, 611–676.
9 X. Yuan, Z. Luo, Q. Zhang, X. Zhang, Y. Zheng, J. Y. Lee and J. Xie, Synthesis of Highly Fluorescent Metal (Ag, Au, Pt, and Cu) Nanoclusters by Electrostatically Induced Reversible Phase Transfer, *ACS Nano*, 2011, **5**, 8800–8808.
10 M. Yu, C. Zhou, J. Liu, J. D. Hankins and J. Zheng, Luminescent Gold Nanoparticles with pH-Dependent Membrane Adsorption, *J. Am. Chem. Soc.*, 2011, **133**, 11014–11017.
11 X. Yuan, M. I. Setyawati, A. S. Tan, C. N. Ong, D. T. Leong and J. Xie, Highly luminescent silver nanoclusters with tunable emissions: cyclic reduction–decomposition synthesis and antimicrobial properties, *NPG Asia Mater.*, 2013, **5**, e39.
12 J. Liu, M. Yu, X. Ning, C. Zhou, S. Yang and J. Zheng, PEGylation and Zwitterionization: Pros and Cons in the Renal Clearance and Tumor Targeting of Near-IR-Emitting Gold Nanoparticles, *Angew. Chem., Int. Ed.*, 2013, **52**, 12572–12576.
13 Y. Yu, Z. Luo, D. M. Chevrier, D. T. Leong, P. Zhang, D.-e. Jiang and J. Xie, Identification of a Highly Luminescent $Au_{22}(SG)_{18}$ Nanocluster, *J. Am. Chem. Soc.*, 2014, **136**, 1246–1249.
14 S. Wang, X. Meng, A. Das, T. Li, Y. Song, T. Cao, X. Zhu, M. Zhu and R. Jin, A 200-fold Quantum Yield Boost in the Photoluminescence of Silver-Doped Ag_xAu_{25-x} Nanoclusters: The 13 th Silver Atom Matters, *Angew. Chem., Int. Ed.*, 2014, **53**, 2376–2380.
15 Y. Chen, D. M. Montana, H. Wei, J. M. Cordero, M. Schneider, X. Le Guével, O. Chen, O. T. Bruns and M. G. Bawendi, Short-wave Infrared in Vivo Imaging with Gold Nanoclusters, *Nano Lett.*, 2017, **17**, 6330–6334.
16 P. L. McEuen, Artificial Atoms: New Boxes for Electrons, *Science*, 1997, **278**(5344), 1729–1730.
17 Z. Luo, X. Yuan, Y. Yu, Q. Zhang, D. T. Leong, J. Y. Lee and J. Xie, From Aggregation-Induced Emission of Au(I)–Thiolate Complexes to Ultrabright Au(0)@Au(I)–Thiolate Core–Shell Nanoclusters, *J. Am. Chem. Soc.*, 2012, **134**, 16662–16670.
18 Y. Chen, T. Yang, H. Pan, Y. Yuan, L. Chen, M. Liu, K. Zhang, S. Zhang, P. Wu and J. Xu, Photoemission Mechanism of Water-Soluble Silver Nanoclusters: Ligand-to-Metal–Metal Charge Transfer *vs.* Strong Coupling between Surface Plasmon and Emitters, *J. Am. Chem. Soc.*, 2014, **136**, 1686–1689.
19 C. A. J. Lin, C. H. Lee, J. T. Hsieh, H. H. Wang, J. K. Li, J. L. Shen, W. H. Chan, H. I. Yeh and W. H. Chang, Synthesis

of Fluorescent Metallic Nanoclusters toward Biomedical Application: Recent Progress and Present Challenges, *J. Med. Biol. Eng.*, 2009, **29**, 276–283.

20 J. Zheng, J. T. Petty and R. M. Dickson, High quantum yield blue emission from water-soluble Au-8 nanodots, *J. Am. Chem. Soc.*, 2003, **125**, 7780–7781.

21 S. Palmal, S. K. Basiruddin, A. R. Maity, S. C. Ray and N. R. Jana, Thiol-Directed Synthesis of Highly Fluorescent Gold Clusters and Their Conversion into Stable Imaging Nanoprobes, *Chem. – Eur. J.*, 2013, **19**, 943–949.

22 M. A. Muhammed, F. Aldeek, G. Palui, L. Trapiella-Alfonso and H. Mattoussi, Growth of in situ functionalized luminescent silver nanoclusters by direct reduction and size focusing, *ACS Nano*, 2012, **6**, 8950–8961.

23 C. Zhou, C. Sun, M. X. Yu, Y. P. Qin, J. G. Wang, M. Kim and J. Zheng, Luminescent Gold Nanoparticles with Mixed Valence States Generated from Dissociation of Polymeric Au(I) Thiolates, *J. Phys. Chem. C*, 2010, **114**, 7727–7732.

24 H. W. Duan and S. M. Nie, Etching colloidal gold nanocrystals with hyperbranched and multivalent polymers: A new route to fluorescent and water-soluble atomic clusters, *J. Am. Chem. Soc.*, 2007, **129**, 2412–2413.

25 K. G. Stamplecoskie, Y.-S. Chen and P. V. Kamat, Excited-State Behavior of Luminescent Glutathione-Protected Gold Clusters, *J. Phys. Chem. C*, 2014, **118**, 1370–1376.

26 Y. Negishi, T. Iwai and M. Ide, Continuous modulation of electronic structure of stable thiolate-protected Au25 cluster by Ag doping, *Chem. Commun.*, 2010, **46**, 4713–4715.

27 H. Qian, D.-e. Jiang, G. Li, C. Gayathri, A. Das, R. R. Gil and R. Jin, Monoplatinum Doping of Gold Nanoclusters and Catalytic Application, *J. Am. Chem. Soc.*, 2012, **134**, 16159–16162.

28 Y. Negishi, K. Munakata, W. Ohgake and K. Nobusada, Effect of Copper Doping on Electronic Structure, Geometric Structure, and Stability of Thiolate-Protected Au25 Nanoclusters, *J. Phys. Chem. Lett.*, 2012, **3**, 2209–2214.

29 G. Soldan, M. A. Aljuhani, M. S. Bootharaju, L. G. AbdulHalim, M. R. Parida, A.-H. Emwas, O. F. Mohammed and O. M. Bakr, Gold Doping of Silver Nanoclusters: A 26-Fold Enhancement in the Luminescence Quantum Yield, *Angew. Chem., Int. Ed.*, 2016, **55**, 5749–5753.

30 S. Wang, Y. Song, S. Jin, X. Liu, J. Zhang, Y. Pei, X. Meng, M. Chen, P. Li and M. Zhu, Metal Exchange Method Using Au25 Nanoclusters as Templates for Alloy Nanoclusters with Atomic Precision, *J. Am. Chem. Soc.*, 2015, **137**, 4018–4021.

31 Y. Negishi, K. Nobusada and T. Tsukuda, Glutathione-protected gold clusters revisited: Bridging the gap between gold(I)-thiolate complexes and thiolate-protected gold nanocrystals, *J. Am. Chem. Soc.*, 2005, **127**, 5261–5270.

32 S. Kumar, M. D. Bolan and T. P. Bigioni, Glutathione-Stabilized Magic-Number Silver Cluster Compounds, *J. Am. Chem. Soc.*, 2010, **132**, 13141–13143.

33 A. Baksi, M. S. Bootharaju, X. Chen, H. Häkkinen and T. Pradeep, $Ag_{11}(SG)_7$: A New Cluster Identified by Mass Spectrometry and Optical Spectroscopy, *J. Phys. Chem. C*, 2014, **118**, 21722–21729.

34 B. R. T. Udaya and T. Pradeep, Luminescent Ag7 and Ag8 Clusters by Interfacial Synthesis, *Angew. Chem., Int. Ed.*, 2010, **122**, 4017–4021.

35 T. K. C. Patrick, L. Marte van der, J. v. H. Elleke, B. Arjan, T. M. R. Marcus, J. K. Abraham, W. B. v. L. Fijs, D. Celso de Mello, J. R. H. Albert and M. Andries, Enhanced luminescence of Ag nanoclusters *via* surface modification, *Nanotechnology*, 2013, **24**, 075703.

36 I. Russier-Antoine, F. Bertorelle, R. Hamouda, D. Rayane, P. Dugourd, Z. Sanader, V. Bonacic-Koutecky, P.-F. Brevet and R. Antoine, Tuning Ag29 nanocluster light emission from red to blue with one and two-photon excitation, *Nanoscale*, 2016, **8**, 2892–2898.

37 F. Aldeek, M. A. H. Muhammed, G. Palui, N. Q. Zhan and H. Mattoussi, Growth of Highly Fluorescent Polyethylene Glycol- and Zwitterion-Functionalized Gold Nanoclusters, *ACS Nano*, 2013, **7**, 2509–2521.

38 L. Shang, R. M. Dorlich, S. Brandholt, R. Schneider, V. Trouillet, M. Bruns, D. Gerthsen and G. U. Nienhaus, Facile preparation of water-soluble fluorescent gold nanoclusters for cellular imaging applications, *Nanoscale*, 2011, **3**, 2009–2014.

39 B. Adhikari and A. Banerjee, Facile Synthesis of Water-Soluble Fluorescent Silver Nanoclusters and Hg-II Sensing, *Chem. Mater.*, 2010, **22**, 4364–4371.

40 L. Shang, S. J. Dong and G. U. Nienhaus, Ultra-small fluorescent metal nanoclusters: Synthesis and biological applications, *Nano Today*, 2011, **6**, 401–418.

41 J. Jiang, C. V. Conroy, M. M. Kvetny, G. J. Lake, J. W. Padelford, T. Ahuja and G. Wang, Oxidation at the Core–Ligand Interface of Au Lipoic Acid Nanoclusters That Enhances the Near-IR Luminescence, *J. Phys. Chem. C*, 2014, **118**, 20680–20687.

42 L. G. AbdulHalim, M. S. Bootharaju, Q. Tang, S. Del Gobbo, R. G. AbdulHalim, M. Eddaoudi, D.-e. Jiang and O. M. Bakr, $Ag_{29}(BDT)_{12}(TPP)_4$: A Tetravalent Nanocluster, *J. Am. Chem. Soc.*, 2015, **137**, 11970–11975.

43 K. Susumu, H. T. Uyeda, I. L. Medintz, T. Pons, J. B. Delehanty and H. Mattoussi, Enhancing the stability and biological functionalities of quantum dots *via* compact multifunctional ligands, *J. Am. Chem. Soc.*, 2007, **129**, 13987–13996.

44 B. C. Mei, K. Susumu, I. L. Medintz, J. B. Delehanty, T. J. Mountziaris and H. Mattoussi, Modular poly(ethylene glycol) ligands for biocompatible semiconductor and gold nanocrystals with extended pH and ionic stability, *J. Mater. Chem.*, 2008, **18**, 4949–4958.

45 X. Dou, X. Yuan, Q. Yao, Z. Luo, K. Zheng and J. Xie, Facile synthesis of water-soluble Au25-xAgx nanoclusters protected by mono- and bi-thiolate ligands, *Chem. Commun.*, 2014, **50**, 7459–7462.

46 E. Oh, K. Susumu, R. Goswami and H. Mattoussi, One-Phase Synthesis of Water-Soluble Gold Nanoparticles with Control over Size and Surface Functionalities, *Langmuir*, 2010, **26**, 7604–7613.

47 X. Yuan, B. Zhang, Z. Luo, Q. Yao, D. T. Leong, N. Yan and J. Xie, Balancing the Rate of Cluster Growth and Etching for

Gram-Scale Synthesis of Thiolate-Protected Au25 Nanoclusters with Atomic Precision, *Angew. Chem., Int. Ed.*, 2014, **53**, 4623–4627.

48 E. Porret, L. Sancey, A. Martín-Serrano, M. I. Montañez, R. Seeman, A. Yahia-Ammar, H. Okuno, F. Gomez, A. Ariza, N. Hildebrandt, J.-B. Fleury, J.-L. Coll and X. Le Guével, Hydrophobicity of Gold Nanoclusters Influences Their Interactions with Biological Barriers, *Chem. Mater.*, 2017, **29**, 7497–7506.

49 G. Palui, F. Aldeek, W. T. Wang and H. Mattoussi, Strategies for interfacing inorganic nanocrystals with biological systems based on polymer-coating, *Chem. Soc. Rev.*, 2015, **44**, 193–227.

50 L. J. Gerenser, K. E. Goppert-Berarducci, R. C. Baetzold and J. M. Pochan, The application of photoemission, molecular orbital calculations, and molecular mechanics to the silver–poly(*p*-phenylene sulfide) interface, *J. Chem. Phys.*, 1991, **95**, 4641–4649.

51 D. Mishra, F. Aldeek, E. Lochner, G. Palui, B. Zeng, S. Mackowski and H. Mattoussi, Aqueous Growth of Gold Clusters with Tunable Fluorescence Using Photochemically Modified Lipoic Acid-Based Ligands, *Langmuir*, 2016, **32**, 6445–6458.

52 Y. Cohen, L. Avram and L. Frish, Diffusion NMR Spectroscopy in Supramolecular and Combinatorial Chemistry: An Old Parameter—New Insights, *Angew. Chem., Int. Ed.*, 2005, **44**, 520–554.

53 K. Salorinne, T. Lahtinen, J. Koivisto, E. Kalenius, M. Nissinen, M. Pettersson and H. Häkkinen, Nondestructive Size Determination of Thiol-Stabilized Gold Nanoclusters in Solution by Diffusion Ordered NMR Spectroscopy, *Anal. Chem.*, 2013, **85**, 3489–3492.

54 K. Pyo, V. D. Thanthirige, K. Kwak, P. Pandurangan, G. Ramakrishna and D. Lee, Ultrabright Luminescence from Gold Nanoclusters: Rigidifying the Au(I)–Thiolate Shell, *J. Am. Chem. Soc.*, 2015, **137**, 8244–8250.

55 A. R. Smith, S. V. Shenvi, M. Widlansky, J. H. Suh and T. M. Hagen, Lipoic Acid as a Potential Therapy for Chronic Diseases Associated with Oxidative Stress, *Curr. Med. Chem.*, 2004, **11**, 1135–1146.

56 L. Trapiella-Alfonso, M. Menéndez-Miranda, J. M. Costa-Fernández, R. Pereiro and A. Sanz-Medel, Nanostructural transformations of silver nanoclusters occurring during their synthesis and after interaction with UV-light, *Mater. Res. Express*, 2014, **1**, 015039.

57 F. Muniz-Miranda, M. C. Menziani and A. Pedone, Influence of Silver Doping on the Photoluminescence of Protected Ag_nAu_{25-n} Nanoclusters: A Time-Dependent Density Functional Theory Investigation, *J. Phys. Chem. C*, 2015, **119**, 10766–10775.

58 R. Juarez-Mosqueda, S. Malola and H. Hakkinen, Stability, electronic structure, and optical properties of protected gold-doped silver $Ag_{29-x}Au_x$ (x = 0–5) nanoclusters, *Phys. Chem. Chem. Phys.*, 2017, **19**, 13868–13874.

59 E. Oh, J. B. Delehanty, L. D. Field, A. J. Mäkinen, R. Goswami, A. L. Huston and I. L. Medintz, Synthesis and Characterization of PEGylated Luminescent Gold Nanoclusters Doped with Silver and Other Metals, *Chem. Mater.*, 2016, **28**, 8676–8688.